# A SUMMARY OF EXPERIMENTS ON NON-STEADY CAVITATION

Performed at the Shipbuilding Laboratory of the Technological University of Delft, Netherlands

by

Ir. M. C. MEIJER

Hydrodynamics Laboratory
California Institute of Technology
Pasadena, California

Internal Memorandum 110.7 August, 1963

Copy No. 12

# TABLE OF CONTENTS

# LIST OF FIGURES

## SUMMARY

In this work the author recollects his main experiences and conclusions concerning non-steady cavitation experiments.

A simple theory is developed, indicating the appearance of an "apparent curvature", which seems to be helpful in the explanation of the occurrence of certain forms of cavitation.

Some photographic examples of non-steady cavity flow are given.

Some information is given about specific trouble, experienced with the water tunnel and a possible cure is proposed.

## Introduction

During the past years, several experiments on non-steady cavitation have been tried in the small cavitation tunnel of the University of Delft. Although interesting observations have been made, no results have been published. The main reason for this fact is, that in the course of the work, serious pressure fluctuations have been detected, which interfered badly with the experiments. The variations of the static pressure in the working section of the tunnel, which were of a periodic nature, caused in extreme cases the cavitation number to vary by over 50%. The frequencies of the fluctuations covered a certain range between 2 and 11 cycles per second. With a peak between 4 and 5 cps. As the frequency range of the experimental set-up, reached between 0 and about 15 cps, it can be easily understood, that former quantitative results have been abandoned.

As there is much demand for experimental evidence and for observations, a summary will be given of some of the experiments which have been performed. The author must apologize for having to write from his memory, as the notes which have been made during the experiments are not at his disposal at the time of writing.

## Experimental Set-Up

The experiments have been performed in a working section with 30 cm height and 15 cm width. The maximum velocity of the flow was about 11 m/sec., the cavitation number was limited primarily by impeller cavitation at approximately $\sigma = 0.15$. The models used, were the same as those used in [1] with the following dimensions:

1. Symmetrical Circular Arc, Maximum Curvature $f_o = 0$ mm.
2. Flat Face, Circular Arc, Maximum Curvature $f_o = 3$ mm.

Both profiles: Chord length = 150 mm.
Span = 150 mm.
Maximum thickness = 6 mm.

The models were fixed at one side to the driver system, which was of simple design (see fig. 1). No scotch yoke has been used, as the sketched system was considered to give a sufficient approximation of a harmonic oscillation. For simplicity, only a pitching movement of the models has been considered; for the same reason the axis of oscillation has been taken at the half chord point. The amplitude of the oscillating part of the angle of incidence could be adjusted in steps of one degree, up to five degrees.

The dynamometer also was kept as simple as possible. It consisted of a rectangular beam with straingages, which have been connected in such a way that two forces and three moments could be measured. In order to obtain reasonable readings of the drag, the beam has been made too narrow, which resulted in severe vibrations of the models within the experimental frequency ranges, for which reason the dynamometer has been replaced by a stiff tube, after the force measurements were finished. Most of the observations have been made in this condition.

## Force Measurements

Measurements of lift, drag and pitching moment have been made with the aid of "Peekel"-dynamical strain indicators and "Sefram" pen recorders. To obtain the phase angles, the variable part of the angle of incidence has been recorded simultaneously. In the cavitating condition, the recordings showed a very non-linear behavior of the forces, which is the only conclusion which can be drawn from this part of the experiments.

## Investigating Geurst's Theory

In his thesis [2], Geurst has given Nyquist diagrams of small variations of long cavities in the case, where the hydrofoil is in pitching oscillation about the center of its chord. In his diagrams the modulus represents the relative amplitude of the variation of the cavity length and the argument represents the phase angle between the oscillatory movement of the hydrofoil and the above-mentioned variations. The curve which

had been computed, was valid for a cavity length equal to three chord lengths. In trying to investigate the results, the following occurred.

1. Cavities of three chord lengths showed variations caused by $\sigma$ fluctuations in the tunnel, which made observations impossible, for this reason a curve for $\ell/c = 1.5$ had been computed by Geurst. At this cavity length ratio, a more stable condition existed.
2. The very small amplitudes, supposed in the theory, could not be measured, so the amplitudes had to be increased.
3. The cavity length variations proved to be very non-linear; nevertheless some rather coarse observations have been performed. The qualitative results are sketched in fig. 2b and 2c, as compared with the theoretical curve sketched in fig. 2a.

The loop in fig 2b proved to be caused by the periodic variation of the pressure in the tunnel.

From this experiment it has been learned, that Geurst's theory must be right when it concludes that up to a certain point the amplitude of the cavity variations decreases with the frequency. Also the existence of loops in the diagram seems to be true.

Differences between experiment and theory are:

(a) The phase angle seems to be larger than prospected,

(b) The position of the loops differ.

These differences may be caused by the fact that much larger amplitudes have been applied than could be allowed by the theory. With partially cavitating conditions, comparative results have been obtained.

Observations of Non-linear Behavior of Cavity Variations

To obtain some insight in the behavior of non-steady cavitation, extensive observations have been made by merely looking at the stroboscopically illuminated cavitation. Most of the observations concern partial cavitation, as in this condition the least trouble was experienced from the $\sigma$ variations in the flow.

Photographic recordings of the cavitation phenomena are included in this report.

The general behavior of the symmetrical hydrofoil is the following: (see photo 1).

1. Starting from zero angle of attack $\alpha$, the cavity grows with increasing $\alpha$ in a manner which conforms to the corresponding stationary conditions.

2. When $\alpha$ begins to decrease, the upstream part of the cavity decreases in thickness, the volume being displaced towards the rear end.

3. With further decrease of $\alpha$, the cavity withdraws towards its middle downstream end when it had covered a nearly square portion of the model. When the extreme length of the cavity had been less than half the span of the model, the cavity splits into nearly square parts.

4. Now the cavity starts to lose volume and disintegrates into a cavitating ring vortex.

5. The cavitating ring vortex seems to be formed in the plane of the suction side of the model. Soon after leaving the trailing edge, the downstream end of the ring vortex is lifted upward, whence the upstream end stays in contact with the model.

6. After the whole ring vortex has left the model, it tends to obtain a vertical position with its axis in the direction of flow.

In nearly any case, also in fully cavitating conditions and when the model never becomes wetted, such cavitating ring vortices can be observed.

A possible explanation of the existence of the ring vortex is given in fig. 3.

Apparent Curvature

Observing the flat skeleton line hydrofoil model at high frequencies of oscillation, small amplitude and low cavitation number, bubble cavitation was detected over the middle portion of the suction side of the model. This phenomenon, which appeared for a very short time during each period of oscillation, gave a picture which was very much the same as that previously noticed with the curved skeleton line model in stationary condition at small angle of attack and low cavitation number (see fig. 4. ).

From this observation the idea was born, that the rotational oscillation might induce an "apparent curvature", which can be explained by observing the local angle of attack of the relative, undisturbed velocity in every point along the chord of the profile. This local relative velocity is composed of the velocity of flow at infinity and of the tangential relative velocity caused by the angular movement of the profile. If in theory the obtained velocity vectors are turned over an angle, equal to the local angle of attack, the mean line of the profile will show a curvature which is dependent on the product of the reduced frequency and the acceleration of the angle of attack. (See Appendix 1). This curvature will be denoted by the name "apparent curvature".

Using this point of view, the N. S. M. B. at Wageningen has been able to explain several cavitation characteristics of ship propellers.

Apart from the "apparent curvature", also an "apparent angle of attack" appears from the theory as a second order effect.

In Appendix 1 the following formulae are derived. The "apparent curvature" to chord ratio is:

$$\frac{f_a}{c} \approx \frac{1}{4} \hat{\alpha}_v \omega \sin \nu t \tag{19}$$

and the apparent increase of the angle of attack is:

$$\alpha_a - \alpha \approx -\frac{1}{6} (\hat{\alpha}_v \omega)^2 \left\{ \alpha_0 - \frac{1}{2} \hat{\alpha}_v \cos \nu t - \alpha_0 \cos 2\nu t + \frac{1}{2} \hat{\alpha}_v \cos 3\nu t \right\} \tag{20}$$

These formulae should be approximately valid for small values of the constant and variable parts of the angle of attack ( $\alpha_0$ , $\hat{\alpha}_v$ ) and for a sufficiently small value of the reduced frequency $\omega$

The following theoretical conclusions can be drawn:

1. In the first part of the cycle ($0 < \nu t < \pi$), when $\alpha$ is increasing, the apparent curvature is positive with its maximum value at $\nu t = \pi/2$ The apparent increase of the angle of incidence is of second order and will be neglected. The effect is that the cavity length will be larger than in the stationary condition.

2. In the second part of the cycle ( $\pi < \omega t < 2\pi$), when $\alpha$ is decreasing, the apparent curvature is negative, with the effect of rapid collapse of the cavity.

3. The results of experiments concerning rotationally oscillating hydrofoils should be plotted on a basis of the product of the amplitude of the angular movement and the reduced frequency, rather than on the reduced frequency alone.

The above conclusions are in full agreement with the experience gained with the experiments.

Kutta Condition

At the Fourth Symposium on Naval Hydrodynamics, held in Washington, D. C. in 1962, some doubt had been expressed by several delegates, about the validity of the Kutta-Condition in non-steady flow. In a trial to throw some light on this problem, a simple experiment has been done in the Delft Cavitation Tunnel.

It is known, that vortices of enough strength are capable of collecting small air bubbles and holding them for some time; in this ventilated condition the vortices are readily visible.

In figure 3 it is shown that the vortices leaving the trailing edge of the model should turn in alternate directions and that there should be a marked difference in height position of these vortices. Now it has been thought, that, if the Kutta-Condition were not valid, also vortices should leave the trailing edge at positions in between those of the normal ones mentioned above, or, because of the infinite velocity around the trailing edge, separation near the trailing edge would occur, with its known aptness to ventilate.

In the experiment, the symmetrical model was driven at high frequencies. The air was supplied from a hypodermic needle-tube. In order to prevent the tube from excessive bending, the velocity of flow had to be low. The ventilated vortices which appeared, had a very marked sinusoidal pattern as seen from aside. No vortices in between and no ventilated separation near the trailing edge of the model could be obtained.

A schematic drawing of the observed wake pattern is shown in fig. 5. It is very difficult to give any conclusion, although no reason could be found to reject the Kutta-Condition.

Stagnation Point at the End of a Full Cavity

Previously the author had concluded that at the rear end of a cavity which partially covers the hydrofoil model, a stagnation point exists [1]

With the oscillating hydrofoil set up it was thought to be possible to obtain an indication of the possible existence of a stagnation point at the rear end of a cavity which exceeds the length of the hydrofoil model. To this end, an electronic pressure transducer was connected to a pressure tap in the centerline of a sidewall of the working section behind the trailing edge of the model. By varying the usual parameters, a condition was established, at which the rear end of the cavity would pass the concerning pressure hole when the angle of incidence was varied slowly.

At the symposium in Washington, D. C. mentioned before, the author had informed the audience, that a recorded rise of the pressure above its static value had indicated the probable existence of a stagnation point in the two dimensional cavity. A repetition of the experiment at a later date gave no confirmation of the earlier observations until in one case, peaks of higher than static pressure again occurred as can be seen in fig. 6.

Photographic Examples

In Appendix 2 some notes are given concerning the technique applied in producing the accompanying photographic examples of non-steady cavity flow. In this summary only a choice of the best examples has been included.

Photo 1 Shows clearly the cavitating vortex ring which is the last phase of the collapsing cavity.

Photos 2 and 3 show the bubble cavitation at an instant of small but increasing angle of attack, probably resulting from the "apparent curvature".

Photo 4 shows the tremendous non-steady behavior at cavity lengths between 0.7 and 1 chord, resulting from fluctuations in the flow. Also in this case where $\alpha$ is constant, except for some elastic vibration, cavitating vortex rings can be clearly seen; the rings seem to originate at the 0.7 chord point.

Photos 5 and 6 show a waving appearance of long cavities at high frequencies of oscillation.

Tunnel Problems

As has been mentioned in Chapter 4 and in the Introductory remarks, much trouble has been experienced by non-steady conditions other than those, directly resulting from the oscillations of the hydrofoil.

As long as the fluctuation frequencies are high, relative to the frequency of the quantity under consideration, it is often possible to find a mean value, which gives a good approximation for the pursued purpose.

In the case described in Chapter 4, where the curve, resulting from the experimental data should have been dependent upon the reduced frequency, most of the covered range was found to be a function of non-reduced frequencies, which very soon proved to be inherent to the tunnel flow.

To investigate the nature of the trouble, two electronic pressure transducers have been connected to several pressure taps, two at a time and the amplitude and the phase of both signals have been compared with the aid of a dual beam oscilloscope. The following results have been obtained.

1. No apparent fluctuation appeared in the velocity head.
2. Amplitude and phase of the pressure fluctuations were nearly identical in all points of the tunnel where the measurements have been carried out. They were independent of the local mean pressure.

The above observations indicated a "breathing" of the whole tunnel caused by the elastic properties of the tunnel walls. To prove

this an electronic displacement transducer has been mounted successively at different points of the tunnel plating; an investigation of the deflections of the stiffeners has been included. The output signal has been compared with the signal from a fixed pressure transducer. The results were as follows:

3. A measurable deflection amplitude has been found at the middle of the straight stiffeners.

4. A relatively large deflection amplitude occurred in the middle of the flat plates.

5. A constant phase connected the deflections with the pressure variations.

As is generally the case with elastic oscillations, three ways are possible to eliminate the trouble:

1. Find the cause of the excitation and remove it.

2. Change the resonance frequency of the system in such a way that no interference with the measurements will be experienced.

3. Apply a damping which suppresses the amplitude of oscillation.

Sub. 1: As possible causes of the excitation, the following have been considered:

1.1 Unsteady flow conditions in the elbows of the tunnel.

This possible cause has been investigated by observing the pressure fluctuations immediately after stopping of the impeller motor. The oscillations died out very soon, but no absolute certainty could be obtained, as the decrease of the velocity of flow was too marked.

1.2 The impeller driving system, consisting of an A. C. motor and a "Hydraulic Variator" with V-belts on either side.

Variations in the rotation velocity have been observed with the aid of a small generator and a low frequency electronic filter. A range of frequencies between some 2 and 6 c/s showed appreciable amplitudes of variation.

1.3 The rubber bearing carrying the impeller shaft inside of the tunnel, has always been very noisy. It was thought, that this bearing could have been of influence on the vibrations mentioned above.

To be able to make a simple visual check of this bearing, the tunnel had to be opened. The bearing was found to be in bad shape and it was decided to replace it by a new bearing of the hydrostatic type. With this it would be reasonably certain that the bearing could be no cause of vibrations.

Sub. 2. The resonant system thought to be composed mainly of the elastic flat sides of the tunnel sections, acting as a spring and the mass of the water, can in principle be changed in two ways:

2.1 Effectively stiffening the tunnel walls, for instance covering the plates with a layer of concrete, or rebuilding the major part of the tunnel, using circular tunnel sections instead of the existing square ones. This stiffening will increase the resonance frequency.

2.2 Reducing the effective stiffness of the tunnel by exchanging at least one of the tunnel sections by one with exaggerated elastic properties. In this way the natural frequency will be reduced.

As is the case in the analogy of radio circuits, it may be worth while to try a reduction of the natural frequency instead of an increase.

Sub. 3. The displacement of the oscillating water mass is possible through the deaerating pipes and in the present case by variation of the water level in the dome which is part of the vacuum system. An effective damping can be obtained by inserting a restriction in the dome. It should be noted however, that any collection of air bubbles or the presence of cavitation decreases the damping again.

In the case of the Delft cavitation tunnel, a restricting plate in the dome effectively suppressed the fluctuations at the lower frequencies. The remaining fluctuations showed a peak at about 20 c/s.

From this it may be concluded that an improvement may be expected when the natural frequency is reduced and an effective damping is made without interfering with the deaerating system; this will be less expensive than increasing the stiffness of the tunnel.

Acknowledgement

The author is indebted to Prof. Ir. J. Gerritsma for the advise given and to G. van Leeuwen and the personnel of the Shipbuilding Laboratory

of the Delft Technological University for their assistance in the execution of the work.

To the Supervisors and Personnel of the Hydrodynamics Laboratory of the California Institute of Technology, the author is indebted for their assistance in the production of this report.

To the "Netherlands Organization for Pure Research, ZWO," the author is indebted for their support, given to the author in order to do research at the facilities of the California Institute of Technology.

## REFERENCES

1. Meijer, Ir. M. C.
"Some Experiments on Partly Cavitating Hydrofoils"
Int. Shipb. Progress, Vol. 6 No. 60, August, 1959.

2. Geurst, J. A.
"Linearized Theory of Two Dimensional Cavity Flows"
Doctor's Thesis, May, 1961.

# APPENDIX I

Simple Theory Concerning the "Apparent Curvature" and the "Apparent Angle of Attack" of a flat plate hydrofoil.

A1. 1. Symbols: (see fig. 5)

$\alpha$ = Momentary angle of attack

$\alpha_o$ = Constant part of angle of attack

$\alpha_v$ = Variable part of angle of attack

$\hat{\alpha}_v$ = Amplitude of $\alpha_v$

$c$ = Chord of profile

$r$ = Radius of point under consideration

$U$ = Velocity of flow at infinity

$V(r)$ = Local relative velocity

$\alpha(r)$ = Local relative angle of attack

$\alpha_a$ = Apparent angle of attack

$f_a$ = Apparent curvature (increase)

$y_1$ = Apparent ordinate of trailing edge

$y_2$ = Apparent ordinate of leading edge

$X$ = Axis through real trailing edge and leading edge

$Y$ = Axis of ordinates.

$\nu$ = Circular frequency of oscillation

$\omega = \frac{\nu c}{2U}$ = reduced frequency of the system

A1. 2.

Consider a point P at the chord of the profile at a distance from the axis of oscillation, (fig. 7a). The relative velocity in P caused by the oscillation of which the acceleration is $\ddot{\alpha}$ , is $r\dot{\alpha}$ perpendicular to the chord, (fig. 7b).

The local relative angle of attack is:

$$\alpha(r) = \alpha + \operatorname{arc\,tg}\left(\frac{r\dot{\alpha}\cos\alpha}{U + r\dot{\alpha}\sin\alpha}\right) \tag{1}$$

Turning the figure over an angle $\alpha(r) - \alpha$ , so, that the relative local velocity vector points in the direction of U and writing $x$ for $r$ , the differential equation for the apparent mean line becomes:

$$\frac{dy}{dx} = -\operatorname{tg}\alpha(r) = -\operatorname{tg}\left\{\alpha + \operatorname{arc\,tg}\left(\frac{x\dot{\alpha}\cos\alpha}{U + x\dot{\alpha}\sin\alpha}\right)\right\} \tag{2}$$

For small angles this is about equal to

$$\frac{dy}{dx} = -\alpha - \frac{x\dot{\alpha}\cos\alpha}{U + x\dot{\alpha}\sin\alpha} \tag{3}$$

The apparent ordinate y at a point x of the mean line becomes:

$$y = -\int_0^x \alpha\,dx - \int_0^x \frac{x\dot{\alpha}\cos\alpha}{U + x\dot{\alpha}\sin\alpha}\,dx =$$

$$= -\alpha x - \int_0^x \frac{\operatorname{ctg}\alpha\; x\,dx}{\frac{U}{\dot{\alpha}\sin\alpha} + x} =$$

$$= -\alpha x - \operatorname{ctg}\alpha \int_0^x x\; d\ln\left(\frac{U}{\dot{\alpha}\sin\alpha} + x\right) =$$

$$= -\alpha x - \operatorname{ctg}\alpha . x \ln\left(\frac{U}{\dot{\alpha}\sin\alpha} + x\right) + \operatorname{ctg}\alpha \int_0^x \ln\left(\frac{U}{\dot{\alpha}\sin\alpha} + x\right) dx \tag{4}$$

$$\ln\left(\frac{U}{\dot{\alpha}\sin\alpha} + x\right) = \ln\frac{U}{\dot{\alpha}\sin\alpha} + \ln\left(1 + \frac{\dot{\alpha}x\sin\alpha}{U}\right) =$$

$$= \ln\frac{U}{\dot{\alpha}\sin\alpha} + \frac{\dot{\alpha}\sin\alpha}{U}x - \frac{1}{2}\left(\frac{\dot{\alpha}\sin\alpha}{U}\right)^2 x^2 + \frac{1}{3}\left(\frac{\dot{\alpha}\sin\alpha}{U}\right)^3 x^3 - \frac{1}{4}\left(\frac{\dot{\alpha}\sin\alpha}{U}\right)^4 x^4 + \ldots. \tag{5}$$

(5) is substituted in (4):

$$y = -\alpha x - \operatorname{ctg}\alpha\left[x \ln\frac{u}{\dot\alpha \sin\alpha} + \frac{\dot\alpha \sin\alpha}{u}x^2 - \frac{1}{2}\left(\frac{\dot\alpha \sin\alpha}{u}\right)^2 x^3 + \frac{1}{3}\left(\frac{\dot\alpha \sin\alpha}{u}\right)^3 x^4 - \dots\right]$$

$$+ \operatorname{ctg}\alpha\left[x \ln\frac{u}{\dot\alpha \sin\alpha} + \frac{\dot\alpha \sin\alpha}{u}\frac{x^2}{2} - \frac{1}{2}\left(\frac{\dot\alpha \sin\alpha}{u}\right)^2 \frac{x^3}{3} + \frac{1}{3}\left(\frac{\dot\alpha \sin\alpha}{u}\right)^3 \frac{x^4}{4} - \dots\right] =$$

$$= -\alpha x - \operatorname{ctg}\alpha\left[\frac{1}{2}\frac{\dot\alpha \sin\alpha}{u}x^2 - \frac{1}{3}\left(\frac{\dot\alpha \sin\alpha}{u}\right)^2 x^3 + \frac{1}{4}\left(\frac{\dot\alpha \sin\alpha}{u}\right)^3 x^4 - \dots\right] \quad (6)$$

At the trailing edge, $x = +\frac{c}{2}$ at the leading edge, $x = -\frac{c}{2}$ so:

$$y_1 = -\alpha\frac{c}{2} - \operatorname{ctg}\alpha \cdot \frac{c}{2}\left[\frac{1}{2}\frac{\dot\alpha c}{2u}\sin\alpha - \frac{1}{3}\left(\frac{\dot\alpha c}{2u}\sin\alpha\right)^2 + \frac{1}{4}\left(\frac{\dot\alpha c}{2u}\sin\alpha\right)^3 - \dots\right] \quad (7)$$

$$y_2 = +\alpha\frac{c}{2} - \operatorname{ctg}\alpha\,\frac{c}{2}\left[\frac{1}{2}\frac{\dot\alpha c}{2u}\sin\alpha + \frac{1}{3}\left(\frac{\dot\alpha c}{2u}\sin\alpha\right)^2 + \frac{1}{4}\left(\frac{\dot\alpha c}{2u}\sin\alpha\right)^3 - \dots\right] \quad (8)$$

The apparent curvature is: $f_a = -\frac{y_2 + y_1}{2}$ (fig. 7c) (9)

$$-\frac{2f_a}{c} = -\frac{1}{2}\operatorname{ctg}\alpha\left[\frac{\dot\alpha c}{2u}\sin\alpha + \frac{1}{2}\left(\frac{\dot\alpha c}{2u}\sin\alpha\right)^3 + \dots\right] =$$

$$= -\frac{1}{2}\frac{\dot\alpha c}{2u}\cos\alpha\left[1 + \frac{1}{2}\left(\frac{\dot\alpha c}{2u}\sin\alpha\right)^2 + \dots\right] \quad (10)$$

The apparent angle of attack is: $\alpha_a \approx \frac{y_2 - y_1}{c}$ (fig. 7c) (11)

$$\alpha_a = \alpha - \frac{1}{2}\operatorname{ctg}\alpha\left[\frac{2}{3}\left(\frac{\dot\alpha c}{2u}\sin\alpha\right)^2 + \frac{2}{5}\left(\frac{\dot\alpha c}{2u}\sin\alpha\right)^4 + \dots\right] =$$

$$= \alpha - \frac{1}{3}\left(\frac{\dot\alpha c}{2u}\right)^2 \sin\alpha\cos\alpha\left[1 + \frac{3}{5}\left(\frac{\dot\alpha c}{2u}\sin\alpha\right)^2 + \dots\right] =$$

$$= \alpha - \frac{1}{6}\left(\frac{\dot\alpha c}{2u}\right)^2 \sin 2\alpha\left[1 + \frac{3}{5}\left(\frac{\dot\alpha c}{2u}\sin\alpha\right)^2 + \dots\right] \quad (12)$$

For small angles $\alpha$ and small values of $\frac{\dot{\alpha} c}{2U}$ equations (10) and (12) yield:

$$\frac{f_a}{c} \approx \frac{1}{4} \frac{\dot{\alpha} c}{2U} \tag{13}$$

and:

$$\alpha_a \approx \alpha - \frac{1}{3} \alpha \left( \frac{\dot{\alpha} c}{2U} \right)^2 \tag{14}$$

These equations can be expressed as a function of the reduced frequency: $\omega = \frac{\nu c}{2U}$ (15)

The oscillation is formulated as:

$$\alpha = \alpha_0 - \hat{\alpha}_\nu \cos \nu t \tag{16}$$

$$\dot{\alpha} = + \hat{\alpha}_\nu \nu \sin \nu t \tag{17}$$

Than is:

$$\frac{\dot{\alpha} c}{2U} = \hat{\alpha}_\nu \frac{\nu c}{2U} \sin \nu t = \hat{\alpha}_\nu \omega \sin \nu t \tag{18}$$

(18) substituted in (13) and (14) gives:

$$\frac{f_a}{c} \approx \frac{1}{4} \hat{\alpha}_\nu \omega \sin \nu t \tag{19}$$

$$\alpha_a - \alpha \approx -\frac{1}{3} \alpha (\hat{\alpha}_\nu \omega)^2 \sin^2 \nu t =$$

$$= -\frac{1}{6} (\alpha_0 - \hat{\alpha}_\nu \cos \nu t)(\hat{\alpha}_\nu \omega)^2 (1 - \cos 2\nu t) =$$

$$= -\frac{1}{6} (\hat{\alpha}_\nu \omega)^2 \left\{ \alpha_0 - \hat{\alpha}_\nu \cos \nu t - \alpha_0 \cos 2\nu t + \hat{\alpha}_\nu \cos \nu t \cos 2\nu t \right\} =$$

$$= -\frac{1}{6} (\hat{\alpha}_\nu \omega)^2 \left\{ \alpha_0 - \hat{\alpha}_\nu \cos \nu t - \alpha_0 \cos 2\nu t + \frac{\hat{\alpha}_\nu}{2} \cos 3\nu t + \frac{\hat{\alpha}_\nu}{2} \cos \nu t \right\}$$

or $$\alpha_a - \alpha \approx -\frac{1}{6} (\hat{\alpha}_\nu \omega)^2 \left\{ \alpha_0 - \frac{\hat{\alpha}_\nu}{2} \cos \nu t - \alpha_0 \cos 2\nu t + \frac{\hat{\alpha}_\nu}{2} \cos 3\nu t \right\} \tag{20}$$

Appendix 2. Photographic Examples.

Camera Test Set-Up:

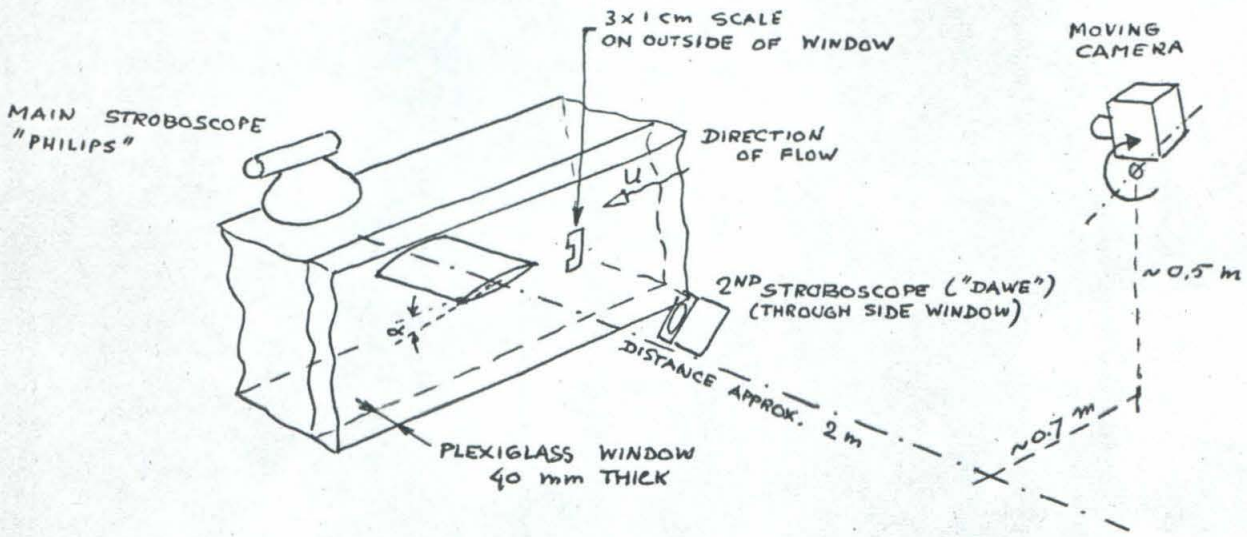


Camers Lens Moved Upwards (as indicated)
Shutter Setting: "B" (surroundings dark)
Diafragm: F/3.5
Film Used: Kodak Panatomic-X (120 roll)
Camera: "Rolleicord"
Main Stroboscope "Philips" (maximum energy)
2nd Stroboscope "Dawe-Strobotorch" (2nd maximum energy)

NOTE: Disturbance In Flow Supposed To Be ~ 20 c/s

## PRINCIPLE OF FLOW MEASUREMENT SET-UP

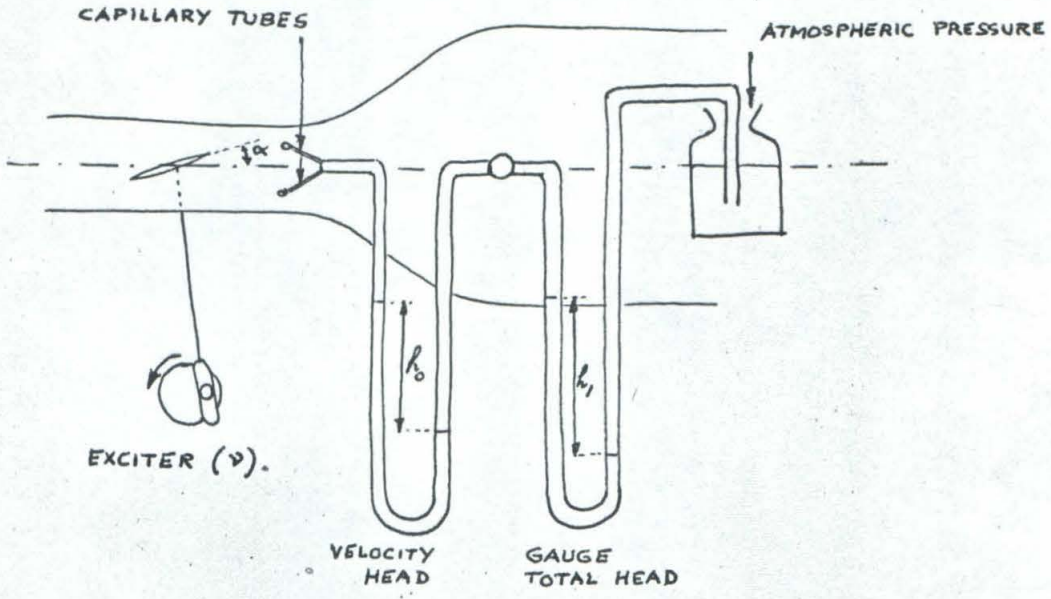


NOTE: The study was meant only to provide visual examples of non-steady cavities; the crude numerical data has been given only to provide the observer of a guide for comparison purposes.

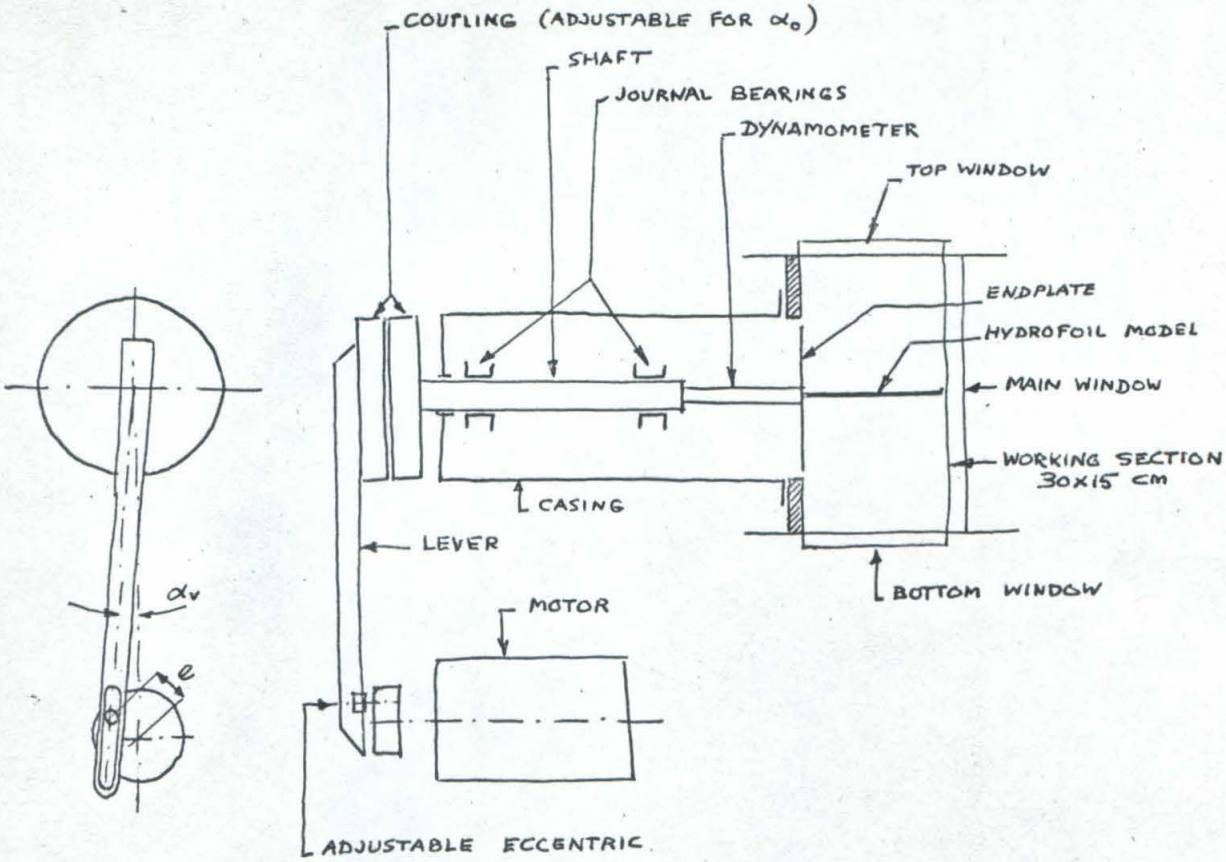


Fig. 1 - Schematic Arrangement of Hydrofoil Driver.

$\bar{\Delta l}$ = Amplitude of variation of cavity length
$l$ = Cavity length
$\nu$ = Circular frequency of driver
$c$ = Model chord
$U$ = Velocity of flow

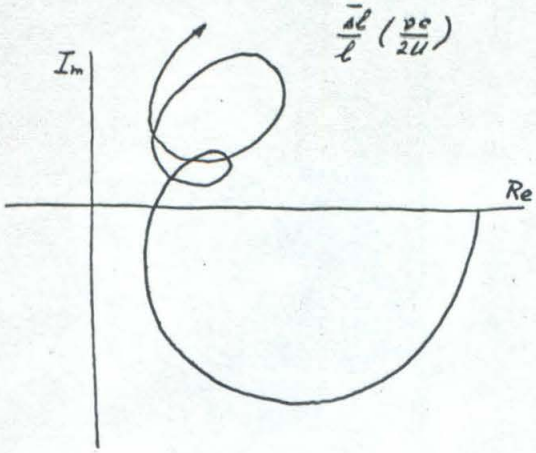


(a) Geurst's diagram (sketched)

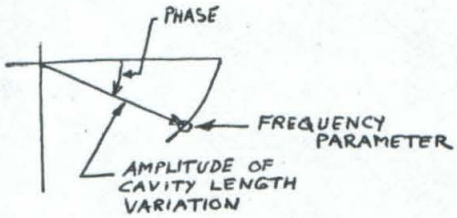


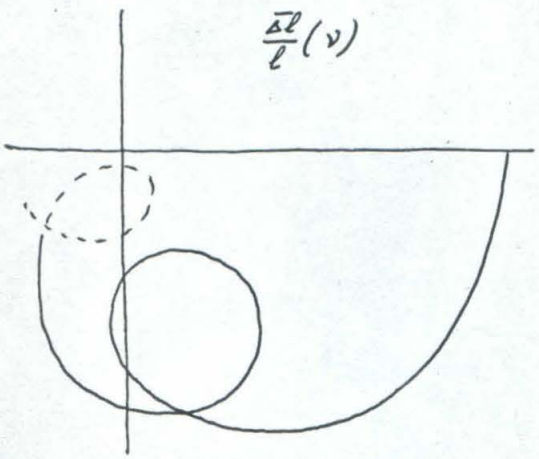


(b) Experimental result depending on $\nu$ only (with free water surface in tunnel dome.)

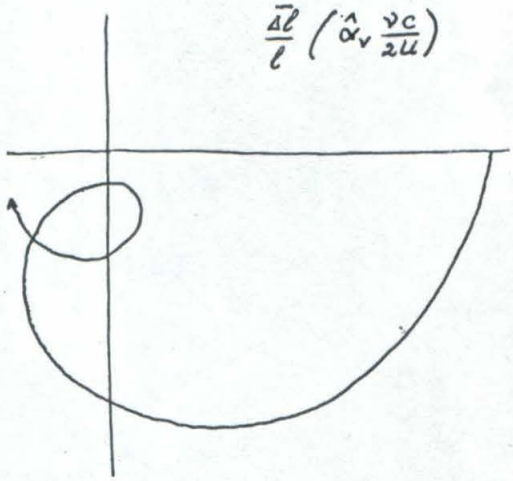


(c) Experimental result depending on $\hat{\alpha}_\nu \frac{\nu c}{2U}$ (with restriction in dome.)

Fig. 2 - Investigation of Results of Geurst's Theory

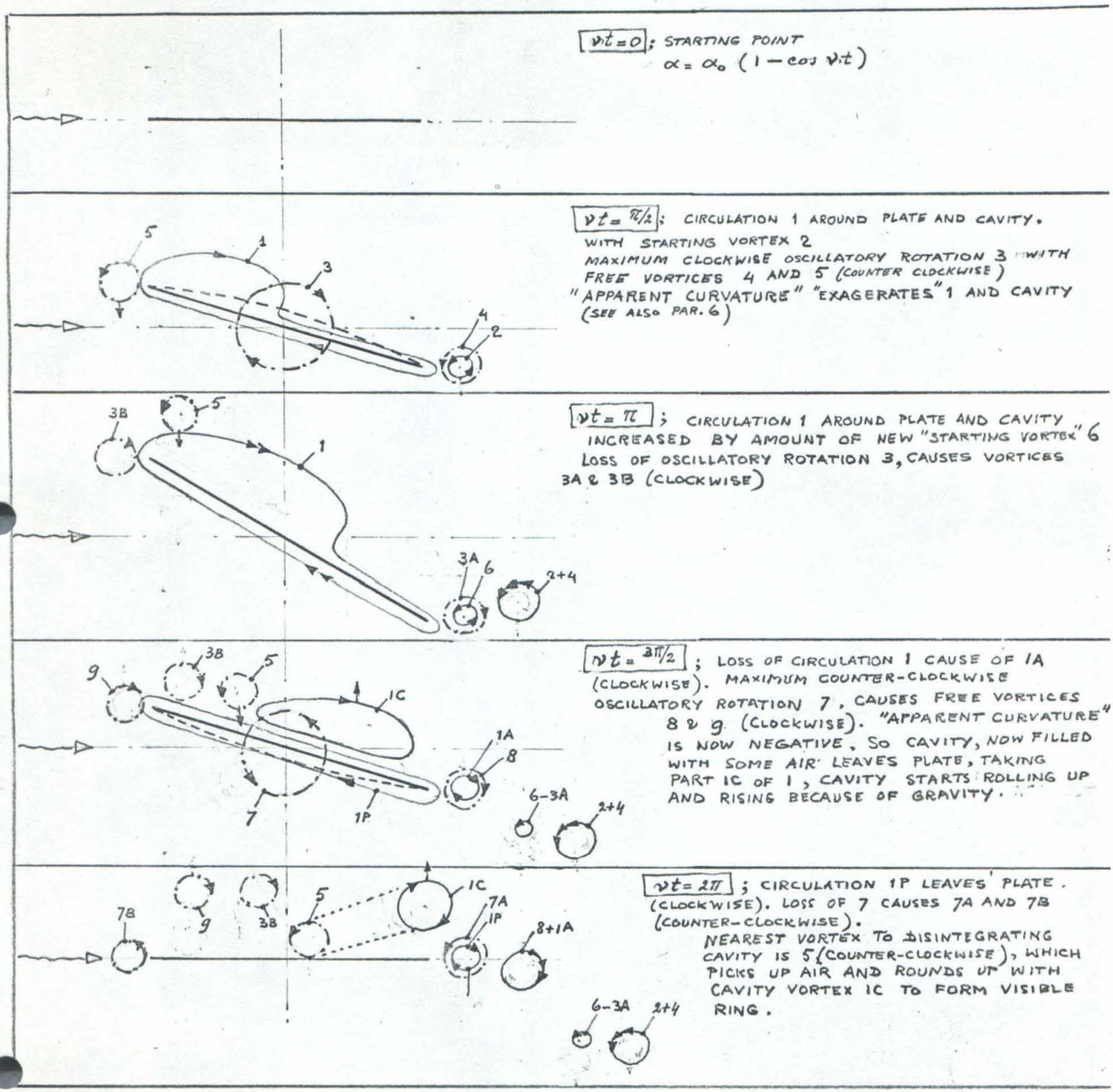


Fig. 3 - Possible Mechanics of Formation of Cavitating Vortex Ring


(a) Hydrofoil with straight mean line, showing bubble cavitation at high oscillation frequency, low $\alpha$ and $\sigma$ values.

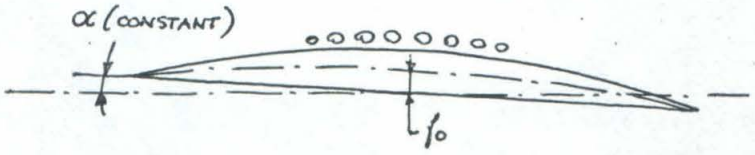


(b) Hydrofoil with curved mean line, showing bubble cavitation at low $\alpha$ and $\sigma$ values in stationary condition.

Fig. 4 - Conformity of Cavitation Appearance on a Hydrofoil Model With Curvature and an Oscillating Hydrofoil Without

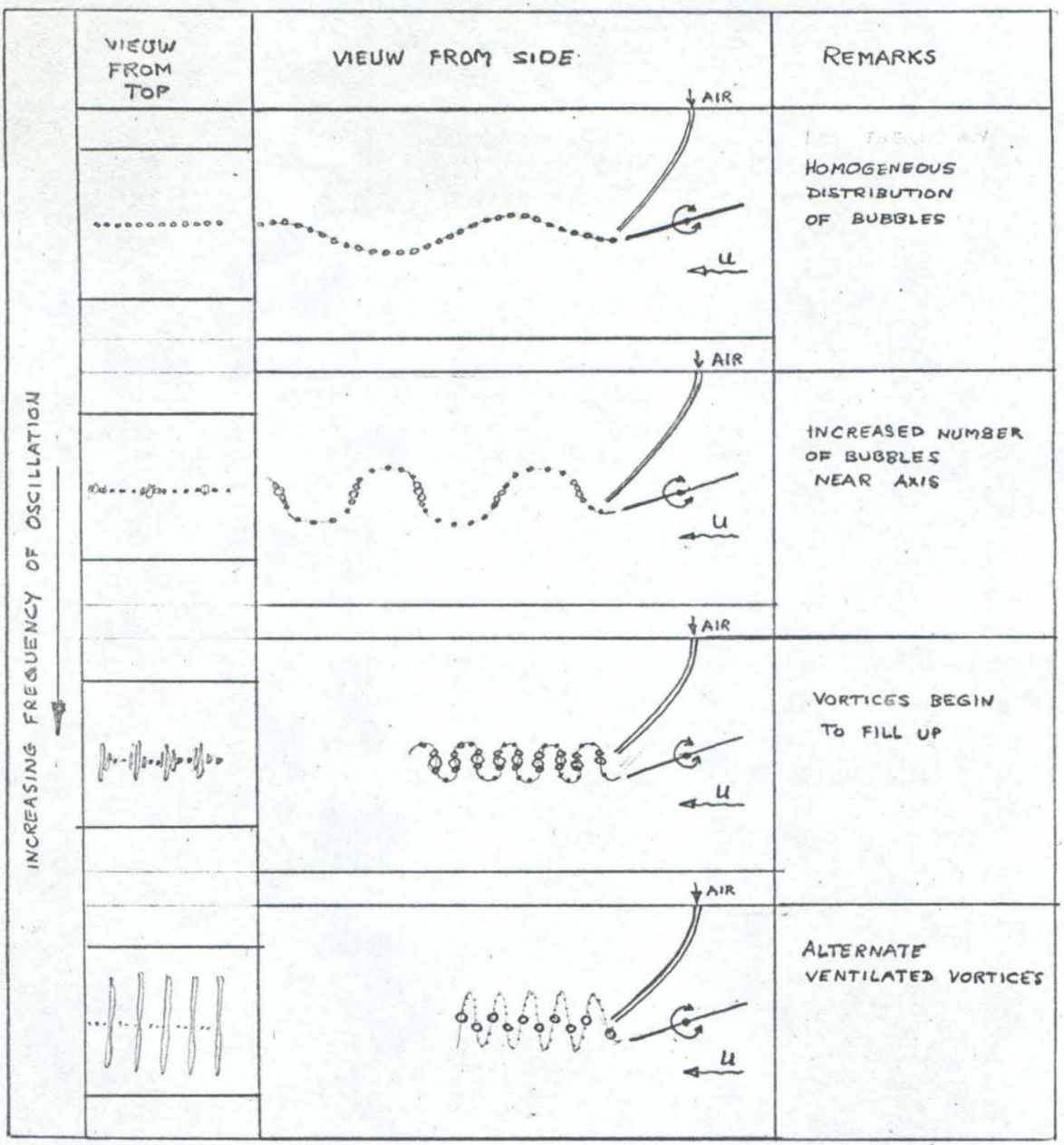


Fig. 5 - Ventilated Wake of Oscillating Hydrofoil

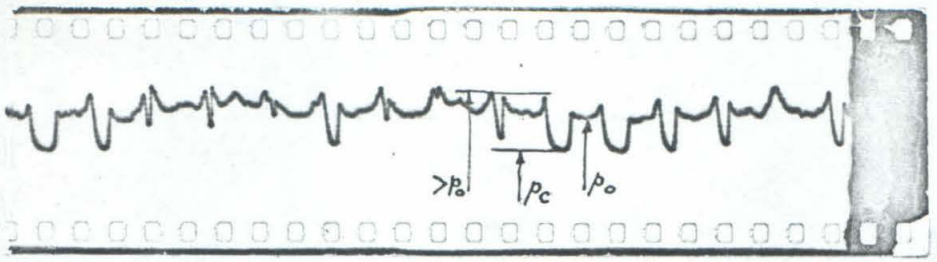


Fig. 6 - Oscilloscope Recording of Pressure at the Rear End of a Slowly Oscillating Full Cavity

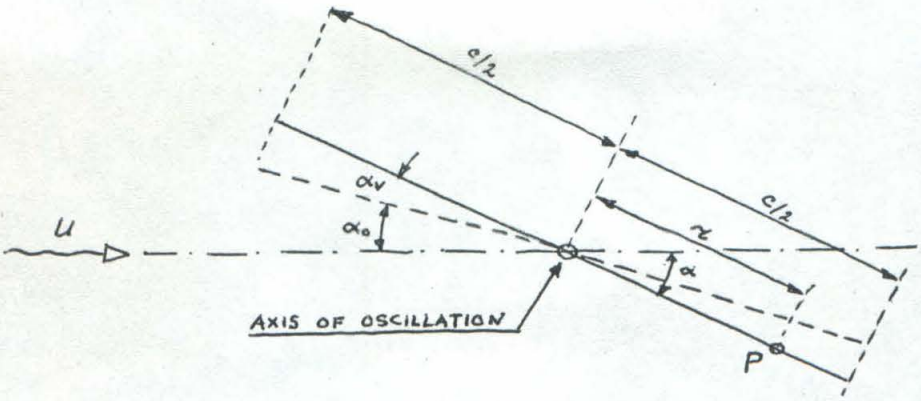


(a) Symbolization (Appendix 1).

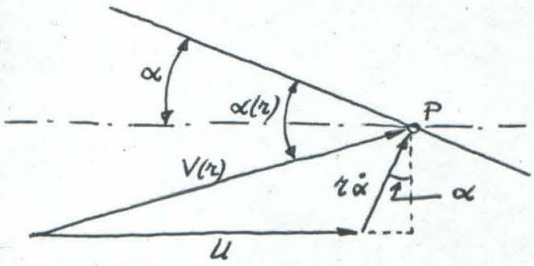


(b) Relative velocity diagram.

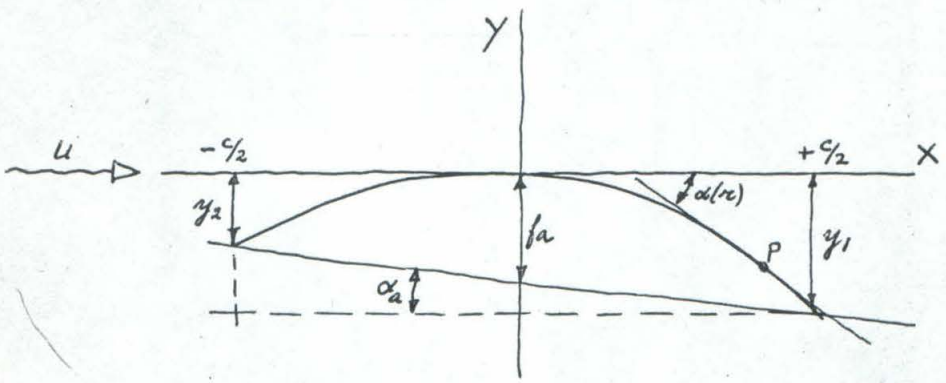


(c) Apparent curvature fa and apparent angle of attack $\alpha_a$.

Fig. 7 - Symbols Used in the Computation of the "Apparent Curvature"

PHOTO 1

Driver Frequency 20.8 c/s
Stroboscope " 18.5 c/s
Velocity 6.84m/s

$$\omega = \frac{\nu c}{2u} = 1.433$$

$$\alpha_o = 3^\circ$$

$$\hat{\alpha}_v = 3^\circ$$

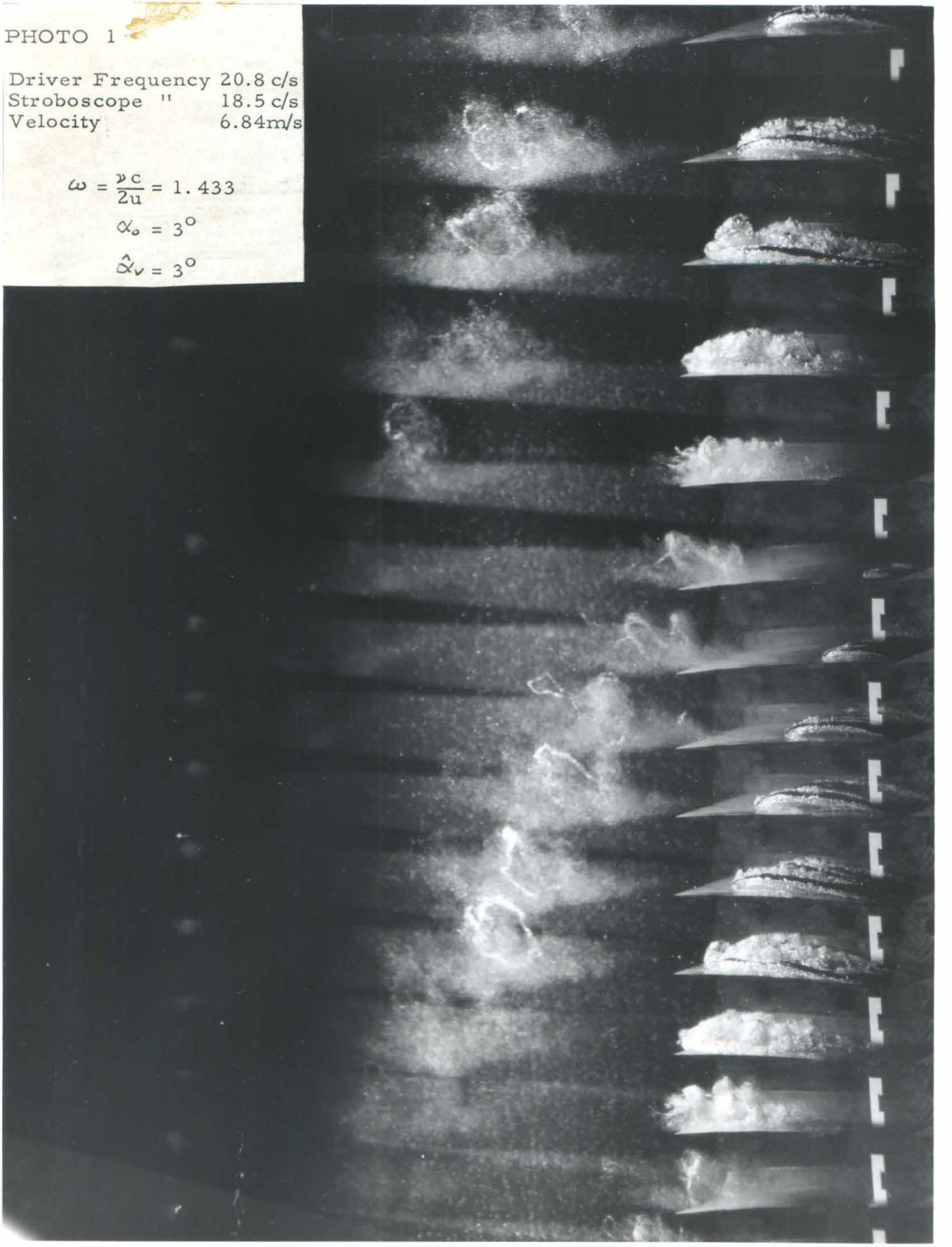

PHOTO 2

Driver Frequency 10.2 c/s
Stroboscope " 9.5 c/s
Velocity 7.90m/s

$$\omega = \frac{\nu c}{2u} = 0.608$$

$$\alpha_o = 3^o$$

$$\hat{\alpha}_v = 3^o$$

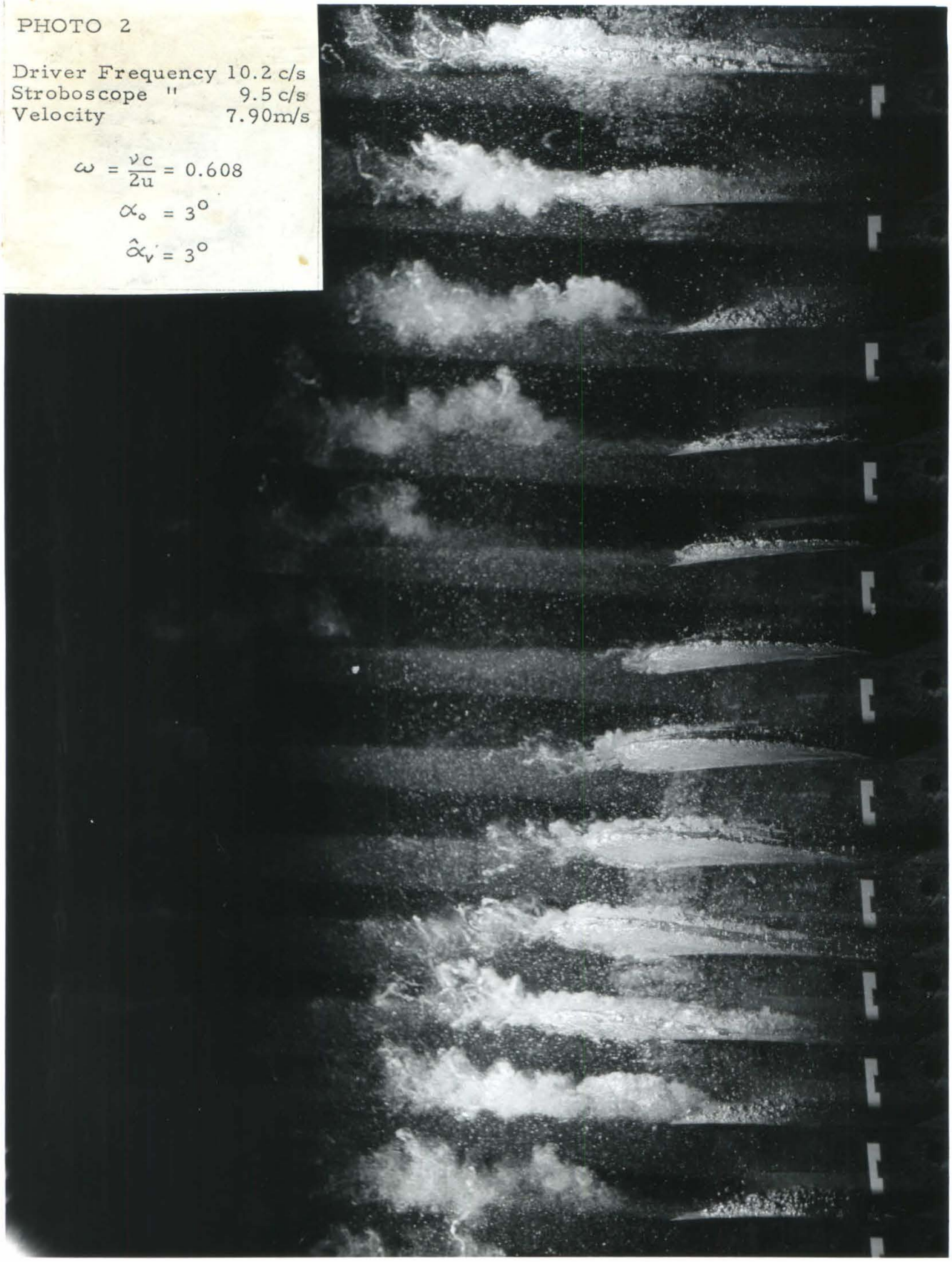

PHOTO 3

Driver Frequency 15.6 c/s
Stroboscope " 14.6 c/s
Velocity 7.90m/s

$$\omega = \frac{\nu c}{2u} = 0.931$$

$$\alpha_0 = 3^\circ$$

$$\hat{\alpha}_v = 3^\circ$$

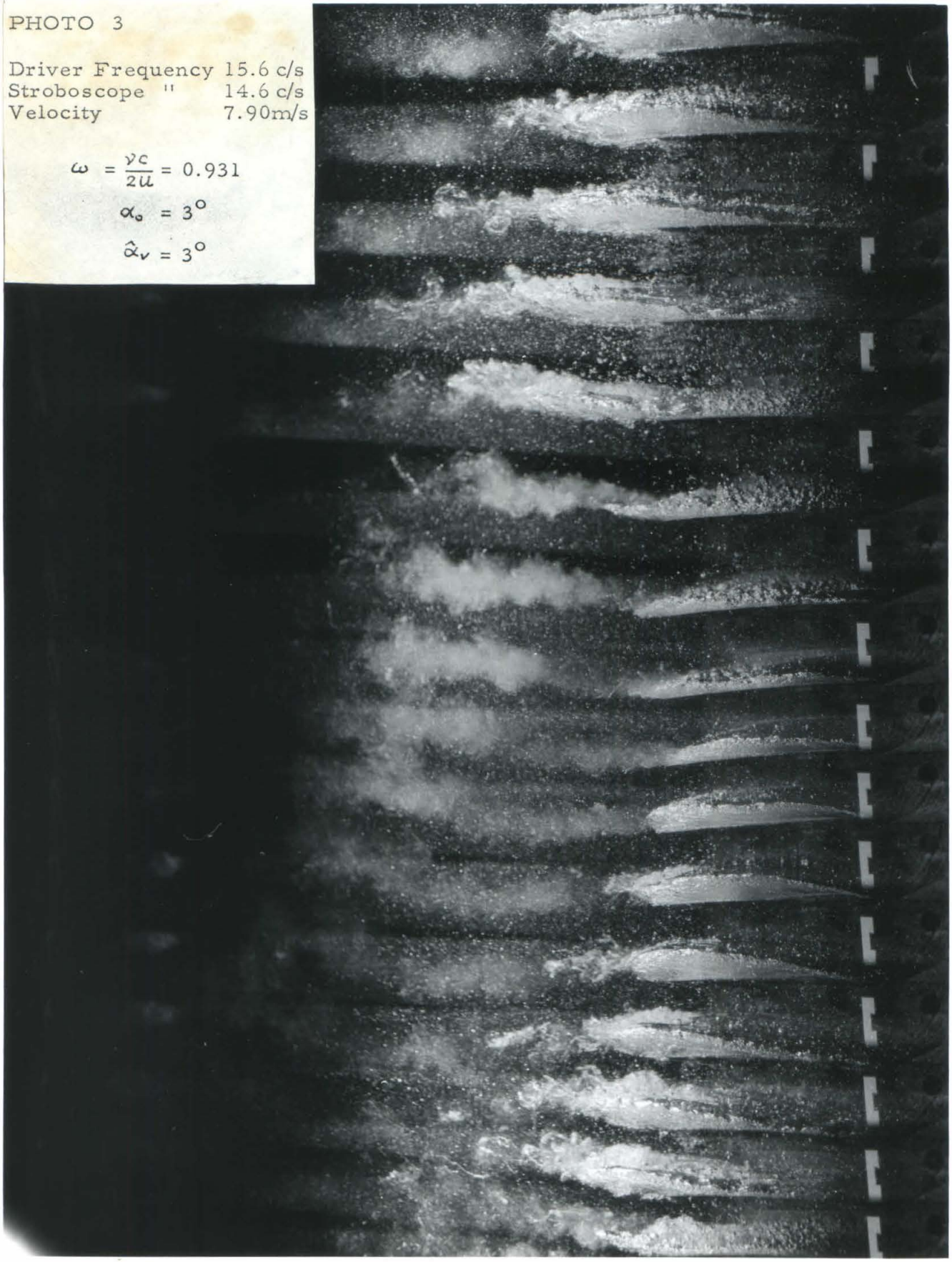

PHOTO 4

Driver Frequency 0 c/s
Stroboscope " 20.4 c/s
Velocity 7.26m/s

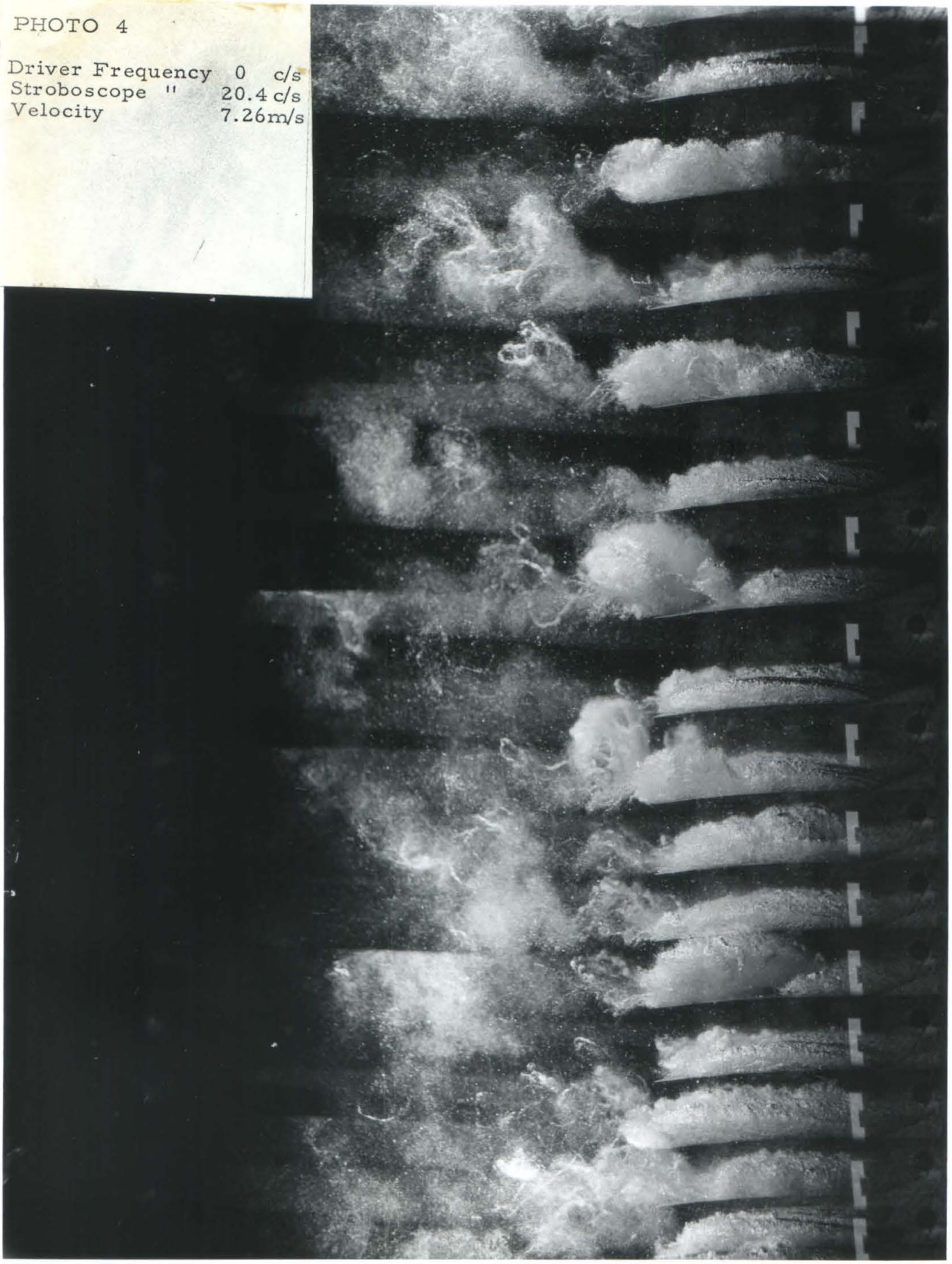

PHOTO 5

Driver Frequency 18.0 c/s
Stroboscope " 16.6 c/s
Velocity 7.50m/s

$$\omega = \frac{\nu c}{2u} = 1.131$$

$$\alpha_o = 6^\circ$$

$$\hat{\alpha}_v = 2^\circ$$

PHOTO 6

Driver Frequency 20.1 c/s
Stroboscope " 18.6 c/s
Velocity 7.50m/s

$$\omega = \frac{\nu c}{2u} = 1.263$$

$$\alpha_o = 6^\circ$$

$$\hat{\alpha}_v = 2^\circ$$

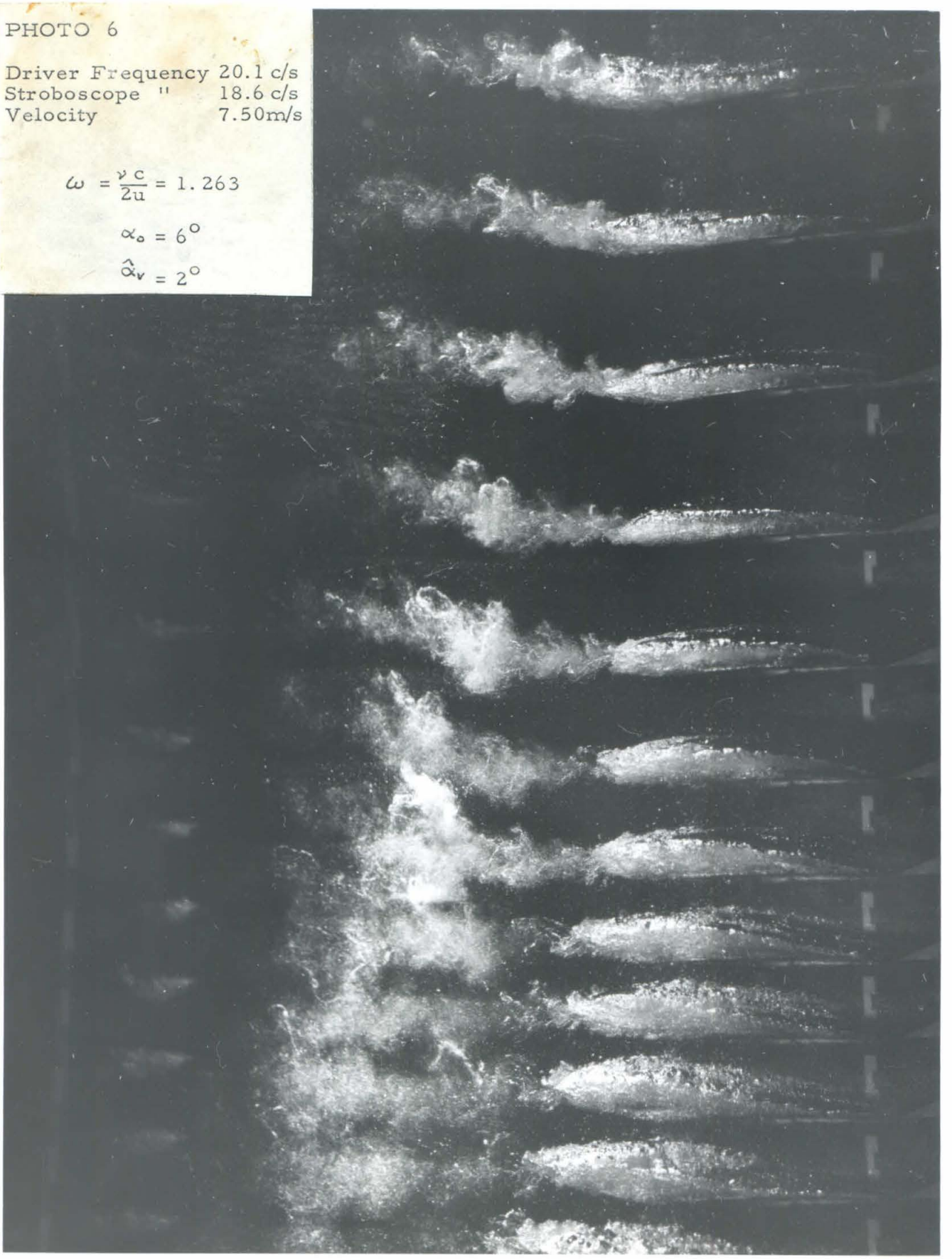

Copy No. 1 - Original Copy - Tunnel Operation Office

2 - File Copy - Hydrodynamics Laboratory Office

3 - Library Copy

4 - Tunnel Operation Office (Working Copy)

5 - Dr. D. A. Jewell, David Taylor Model Basin, Washington 7, D. C.

6 - Dr. D. A. Jewell, c/o University of California, Berkeley, California

7 - 8 - Shipbuilding Laboratory of the Technological University, Mekelweg 2, Delft, The Netherlands

9 - Ir. M. C. Meijer

10 - 11 Supernumerary Copies